MR Imaging of Syringomyelia and Hydromyelia

Benjamin C. P. Lee, Robert D. Zimmerman, John J. Manning and Michael D. F. Deck

AJNR Am J Neuroradiol 1985, 6 (2) 221-228
http://www.ajnr.org/content/6/2/221

MR Imaging of Syringomyelia and Hydromyelia

Benjamin C. P. Lee[1]
Robert D. Zimmerman
John J. Manning
Michael D. F. Deck

The relative effectiveness of plain computed tomography (CT), metrizamide CT, conventional myelography, and magnetic resonance (MR) imaging was compared for the examination of cystic spinal cord lesions. Intramedullary cavities in 18 patients were demonstrated by MR imaging: cavities were uncomplicated in 13 patients, associated with spinal tumors in two, and studied after occipital craniectomy for treatment of Chiari malformation and syringomyelia in two. Cavities were shown by MR imaging in all enlarged spinal cords, but a cavity was shown in only one of four small cords. The rostral limits of the cavities were demonstrated better than were the caudal extensions. Ventricular communication was not demonstrated. Chiari malformation was shown only in cavities that did not involve the medulla. Syringes associated with tumor were indistinguishable from uncomplicated cavities, but the tumor had abnormal signal on long spin-echo sequences in two cases. Cystic cord tumor (one case) had an inhomogeneous appearance. Caudal displacement of the cerebellar hemisphere through the surgical defect associated with compression of the fourth ventricle was shown in two cases after posterior fossa craniectomy. Thirteen patients were studied with metrizamide CT also. MR imaging proved to be as accurate as metrizamide CT in the diagnosis of intramedullary cavities that result in spinal cord enlargement, but it was less sensitive in detecting cavities within normal-sized or diminished spinal cords. It had the advantage that tumor tissue could be distinguished from associated syrinx cavities by differences in signal characteristics; and cerebellar ectopia was evaluated easily on sagittal MR views.

Intramedullary cavities have insidious clinical presentations and usually are indistinguishable from intrinsic tumors [1–5]. The treatment of these two lesions is different: tumors are usually best treated by radiotherapy, certain syringes by surgical decompression, and cavities that communicate with the ventricles, by ventricular shunt procedures [1, 2, 4–9]. Plain computed tomographic (CT) scans sometimes reveal an enlarged cervical cord and associated cavity within, but cannot be relied on to be precise in diagnosis, and are almost never helpful in determining whether the cavities communicate with the ventricular system [10–15]. Thoracic cord cavities also are seldom demonstrated because of poor resolution and artifact. The only methods currently available for confirmation are metrizamide myelography and CT with intrathecal metrizamide. Both demonstrate cord enlargement, and CT, especially after a delay of 8–24 hr, often reveals filling of the cavities [11, 14–16]. The spinal cord can be demonstrated using magnetic resonance (MR) imaging, and there is evidence that MR imaging is useful in the diagnosis of syringomyelia and hydromyelia [17–20]. We attempted to examine its usefulness relative to plain CT, metrizamide CT, and conventional myelography.

Subjects and Methods

We studied 18 patients with intramedullary cavities: 13 represented uncomplicated syringes, three were associated with spinal tumors (glioma, ependymoma, and meningioma

This article appears in the March/April 1985 issue of *AJNR* and the June 1985 issue of *AJR*.

Received June 27, 1984; accepted after revision October 29, 1984.

[1] All authors: Department of Radiology, New York Hospital–Cornell Medical Center, 525 E. 68th St., New York, NY 10021. Address reprint request to B. C. P. Lee.

***AJNR* 6:221–228, March/April 1985**
0195–6108/85/0602–0221

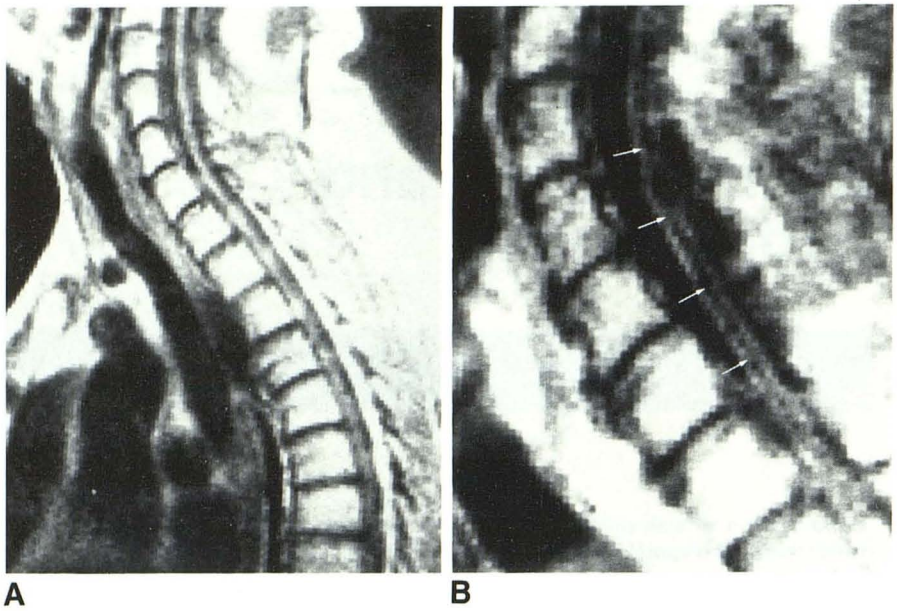

Fig. 1.—Sagittal SE 500/30 images in two patients. **A**, Small size of spinal cord. **B**, Intramedullary cavity (*arrows*).

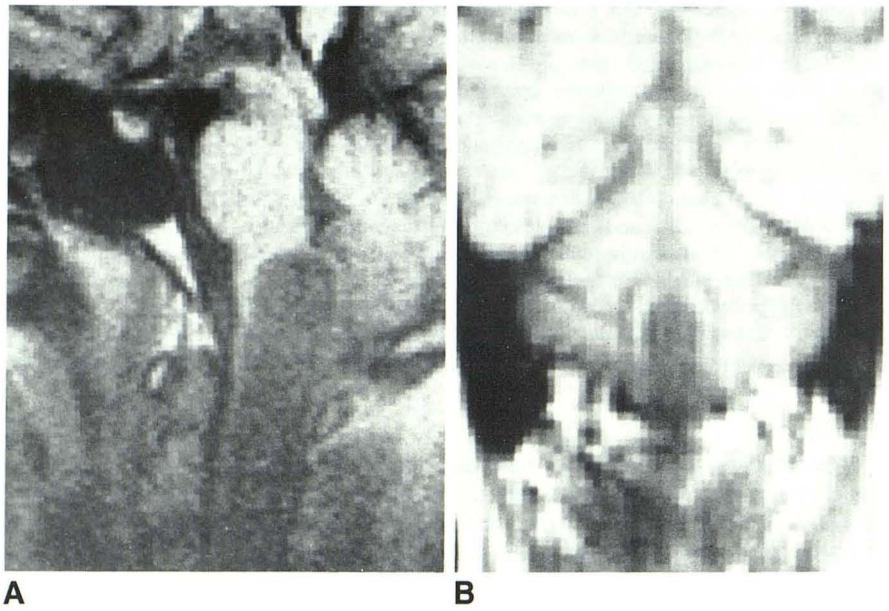

Fig. 2.—SE 500/30 images in two patients. **A**, Sagittal view. Extension of intramedullary cavity into pontomedullary junction. Rounded appearances of cavity and expansion of brainstem. **B**, Coronal view. Slight distortion of fourth ventricle. Ventricular communications are not shown in either case.

treated by surgery and radiotherapy), and two represented hydromyelia that had been treated previously by occipital decompression of associated Chiari I malformations.

MR imaging was performed with a Technicare 0.5 T scanner: a head coil was used for examinations of the upper cervical area and a body coil for examination of the rest of the spine. An initial series of sagittal scout localization views with different spatial offset from a presumed midline position was performed using a spin-echo (SE) technique with an echo time (TE) of 30 msec and repetition time (TR) of 200 msec (SE 200/30). True midline sagittal sections were selected from these views, and multisection coronal scans were obtained routinely in all cases using an SE 500/30 technique. Multisection axial scans were obtained in four cases. One hundred ninety-two gradient steps in the *Y* axis and 256 steps in the *X* axis were used for the scans, corresponding to matrix pixel sizes of 1.3 × 0.98 mm and 2.6 × 1.96 mm for the head and body coils, respectively. The sections were about 10 mm thick. An average of two signals per projection was used to generate the images. A scanning time of 6.6 min was considered appropriate and the images produced were of diagnostic quality. Increased signal-averaging produced scans with better signal-to-noise characteristics, but the prolonged scanning time was judged to be impractical for clinical imaging. SE scans using longer TEs and TRs (SE 2000/60, SE 2000/120) were also obtained in many cases. Other techniques, SE 1500/90 and inversion recovery (IR) 1500/450, were tried in a few initial cases to determine the utility of these additional sequences, but they were not used subsequently as they

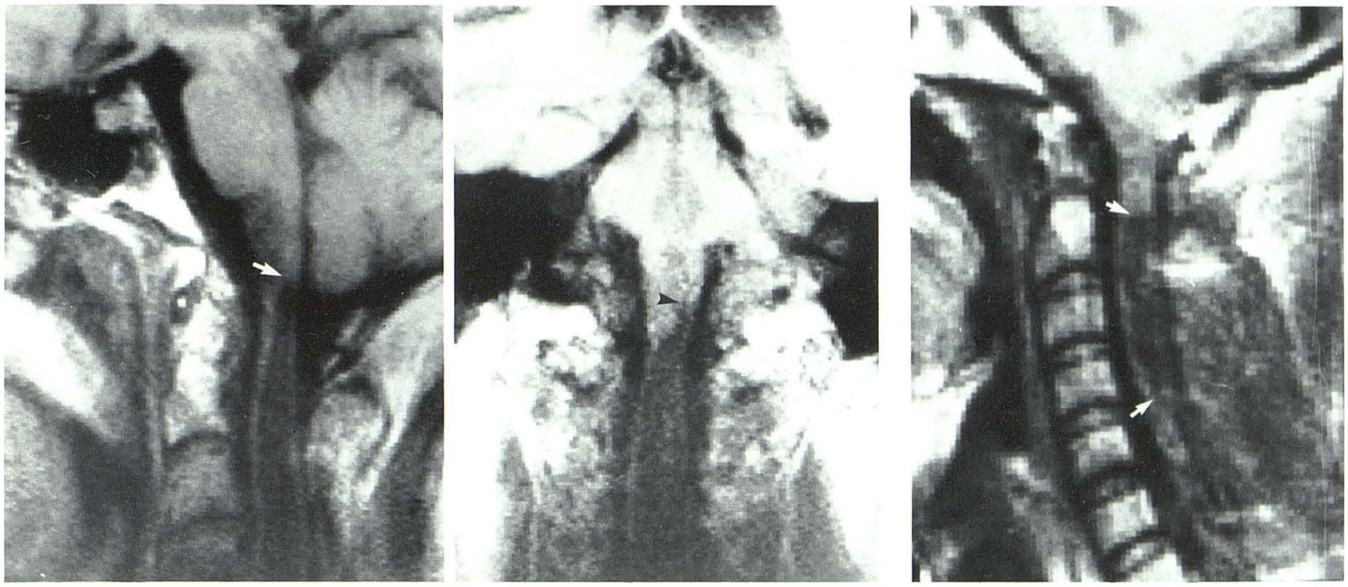

Fig. 3.—SE 500/30 images in two patients. **A**, Sagittal view. Intramedullary cavity extends into cervicomedullary junction (*arrow*). **B**, Coronal view. Intramedullary cavity with tapered upper margin, slightly off midline (*arrowhead*). Ventricular communication is not shown, but small channel cannot be excluded.

Fig. 4.—Sagittal SE 500/30 image. Intramedullary cavity of cervical spinal cord. Upper and lower limits (*arrows*).

failed to demonstrate syringes.

All CT studies except one were performed using a GE 8800 scanner. One patient was examined with a GE 9800 scanner. Contiguous sections of 5 mm thickness were obtained in the cervical regions and 5 or 10 mm sections were obtained in the thoracic regions. Plain CT scans were obtained in all cases. Metrizamide CT scans were obtained immediately after myelography and after delays of 12–24 hr in 13 cases. Pantopaque myelography was performed in one patient in whom metrizamide CT was not performed.

Results

Uncomplicated Intramedullary Cavities

The spinal cords were enlarged in nine and diminished in four cases (fig. 1). Cervical cord enlargement was shown on both sagittal and coronal views. The thoracic cords were clearly demonstrated in only six cases. The margins of the cord were evaluated best by SE 500/30 using four signal averages in the head coil. Metrizamide CT confirmed the spinal cord sizes shown on MR imaging.

Intramedullary cavities were demonstrated by MR in all nine cases in which the spinal cords were enlarged, but only in one with a small cord (fig. 1). SE 500/30 was the optimal technique for demonstrating the cavities. Sagittal and coronal views defined the rostral extent of the cavities in the same cases: two within the medulla (fig. 2), four at the medullocervical junction (fig. 3), and three at the upper part of the cervical cord. The caudal limit of the cavities in the thoracic region was better shown on coronal than sagittal views: two were in the lower cervical cord (fig. 4) and three in the thoracic cord (fig. 5). The caudal limits of the other five cavities were not seen. The rostral margins of the two cavities within the medulla were rounded; cavities that appeared to terminate in the medullocervical junction (four cases) and the cervical cord (four cases) all had tapered shapes (figs. 2–4). The shape of the cavity alone did not appear to be useful in distinguishing uncomplicated cavities from those associated with spinal tumor. No definite communication with the fourth ventricle was demonstrated in any case. Axial views showed the cavities to be central in location within the spinal cord and had homogeneous low signal on SE 500/30 images in all four cases so studied. SE 2000/120 images did not demonstrate the cavities and did not show increased signal in any part of the spinal cord to suggest an associated tumor.

Chiari I malformation shown in five cases and the ectopic tonsils were clearly demarcated from the spinal cord (fig. 6). This malformation was present only in cases where the intramedullary cavities appeared not to enter into the medulla. The two cases of syringobulbia did not have tonsillar ectopia.

A definite cervical intramedullary cavity was shown on one plain CT scan obtained with the GE 9800 scanner (fig. 7). Metrizamide CT showed filling of the intramedullary cavities in four of six cases with expanded spinal cords (fig. 8). Similar filling was seen in three of the four cases of small cords studied (fig. 9). There was cord enhancement in the other case; it outlined a central cavity not filled with contrast material (fig. 10).

Tumor Cysts

Cord enlargement was shown by SE 500/30 in all three cases and abnormal signal of the tumors was shown by SE

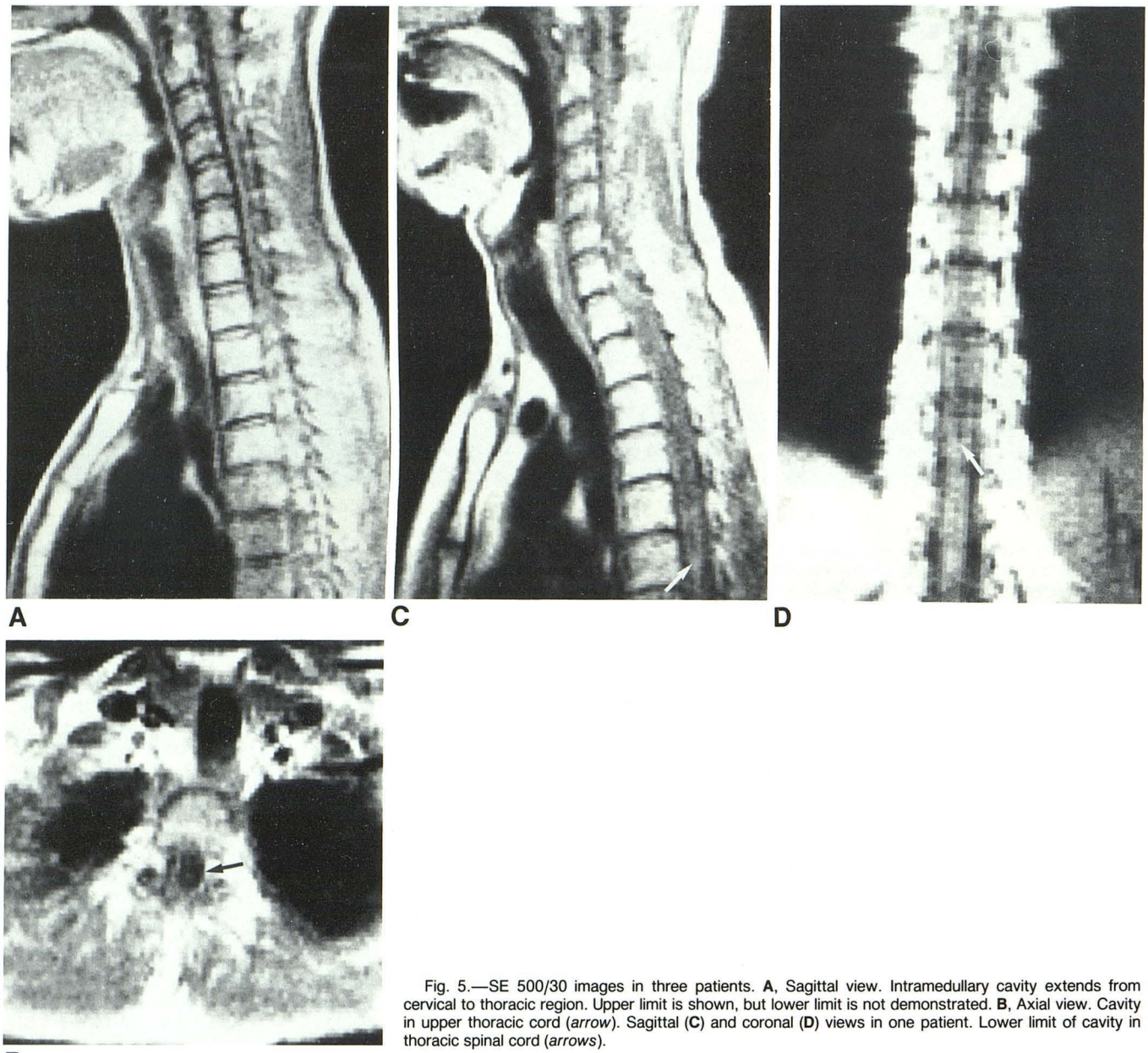

Fig. 5.—SE 500/30 images in three patients. **A**, Sagittal view. Intramedullary cavity extends from cervical to thoracic region. Upper limit is shown, but lower limit is not demonstrated. **B**, Axial view. Cavity in upper thoracic cord (*arrow*). Sagittal (**C**) and coronal (**D**) views in one patient. Lower limit of cavity in thoracic spinal cord (*arrows*).

2000/120 in two cases: A large syrinx cranial to the meningioma was demonstrated on the sagittal SE 500/30 view in one case. A small syrinx associated with an ependymoma was confirmed by surgical exploration in another case (fig. 11). In the third case a cyst causing expansion of the medulla was shown on a sagittal SE 500/30 image; the cervical cord was also enlarged but was separated from the medulla by a normal-sized segment. Axial SE 500/30 and SE 2000/90 images revealed inhomogeneous signal within the intramedullary cavity suggesting cystic as well as solid components (fig. 12). All MR findings were verified by surgery. Metrizamide was not shown within the cavities on delayed CT in any case.

Postoperative Cases

The cervical cord was atrophic in one case and normal in the other. The Chiari I malformations were modified by occipital craniectomy in one case; the entire cerebellum appeared to have descended into the surgical defect and the fourth ventricle appeared small (fig. 13).

Discussion

The diagnosis of syringomyelia or hydromyelia is made only when the intramedullary cavity is imaged. The spinal cord is

Fig. 6.—Sagittal SE 500/30 image. Chiari I malformation. Cerebellar tonsils (*arrowheads*) are clearly distinguished from cervical spinal cord. Termination of intramedullary cavity at upper cervical level.

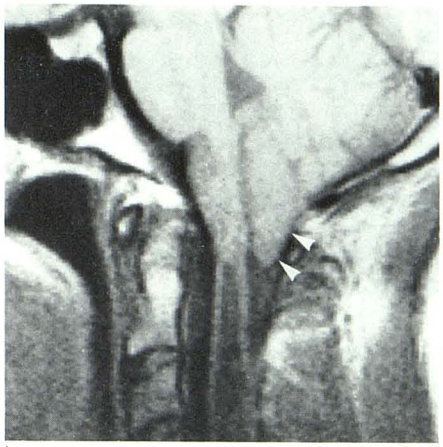

6

Fig. 7.—Plain CT scan using GE 9800 scanner. Intramedullary cavity within enlarged cervical spinal cord. s = subarachnoid space.

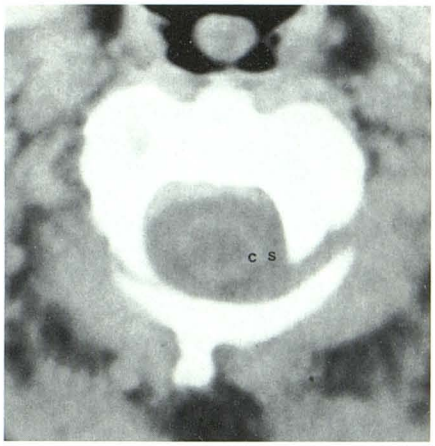

7

8

9

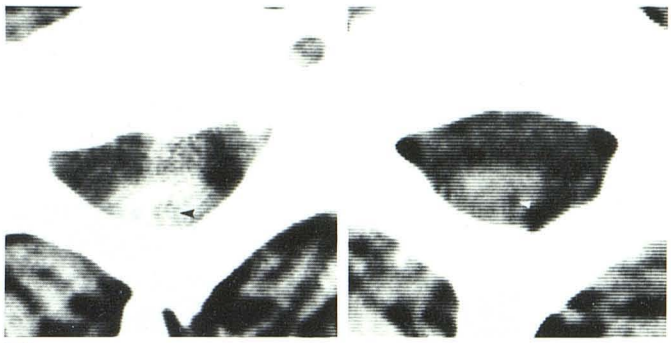

10

Fig. 8.—24 hr delayed metrizamide CT scan. Filling of cavity within enlarged spinal cord.

Fig. 9.—8 hr delayed metrizamide CT scan. Filling of intramedullary cavity (*arrow*) within atrophic spinal cord outlined by contrast material.

Fig. 10.—24 hr delayed metrizamide CT scans at two cervical levels. Spinal cord with higher density than subarachnoid space. Small intramedullary cavity apparently is not opacified with contrast material (*arrowheads*).

often enlarged, but at times it may be smaller than normal [2, 11, 15, 16, 21]. The size of the cord may be evaluated by myelography or metrizamide CT, and occasionally by plain CT of the cervical region [3, 10–16]. Intramedullary cavities are rarely demonstrated on plain CT and often require delayed metrizamide CT examinations [11, 14–16].

A common associated abnormality of hydromyelia is the Chiari I malformation, which has been suggested to play an important part in the pathogenesis of intramedullary cavities [1, 2, 9, 22–24]. The presence of such an anomaly and ventricular communication of the hydromyelia has an important bearing on surgical therapy. Ventricular decompression of cysts that do not communicate with the ventricle in the presence of a Chiari I malformation does not ameliorate the clinical symptoms and often makes them worse [1, 2, 4, 5, 7–9, 25, 26]. Other causes of syringes such as tumor, radiation therapy, trauma, and hemorrhages have to be sought, as these primary diseases also affect therapy [1, 3, 24, 25].

Spinal Cord Size

Intramedullary cavities are not always associated with enlarged spinal cord. MR demonstrates changes in spinal cord size in the cervical region, but is not as sensitive as myelography or metrizamide CT in revealing slight alterations. The presence of kyphosis and scoliosis makes it difficult to align MR sections accurately in the thoracic region in a substantial proportion of cases, and results in poor imaging of the thoracic spine. The smaller diameter of head compared with the body coil also permits better resolution in imaging of the upper cervical spinal and craniocervical junction than is obtained in the rest of the spinal cord using the body coil. SE 500/30 is the optimal pulse sequence for demonstrating the spinal cord. On the whole, sagittal sections are superior to coronal views. Evaluation of spinal cord size is by visual impression, as currently the resolution of MR is inadequate for accurate quantitative measurements.

It has been suggested that spinal cord size is dependent

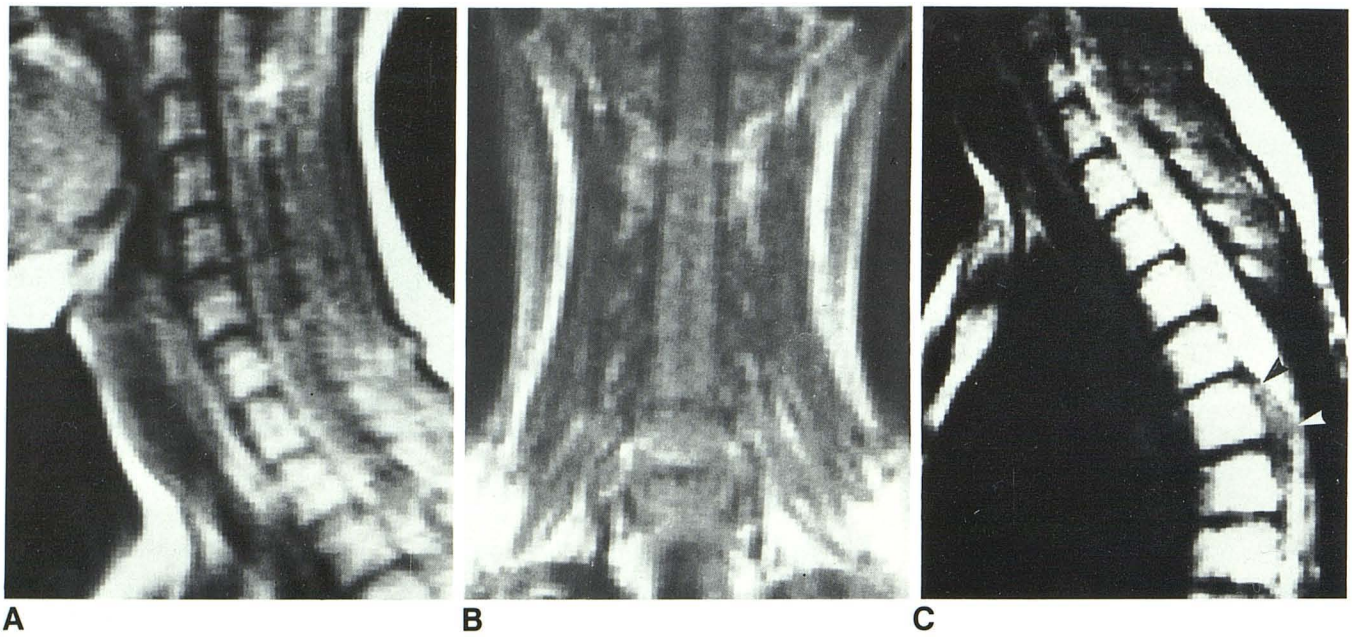

Fig. 11.—Ependymoma. Sagittal (**A**) and coronal (**B**) SE 500/30 images. Intramedullary cavity of cervical spinal cord. **C**, Sagittal 2000/120 image. Generalized increased signal of spinal cord, with area of normal signal anteriorly in upper thoracic cord (*arrowheads*). Intramedullary cavity is no longer visible.

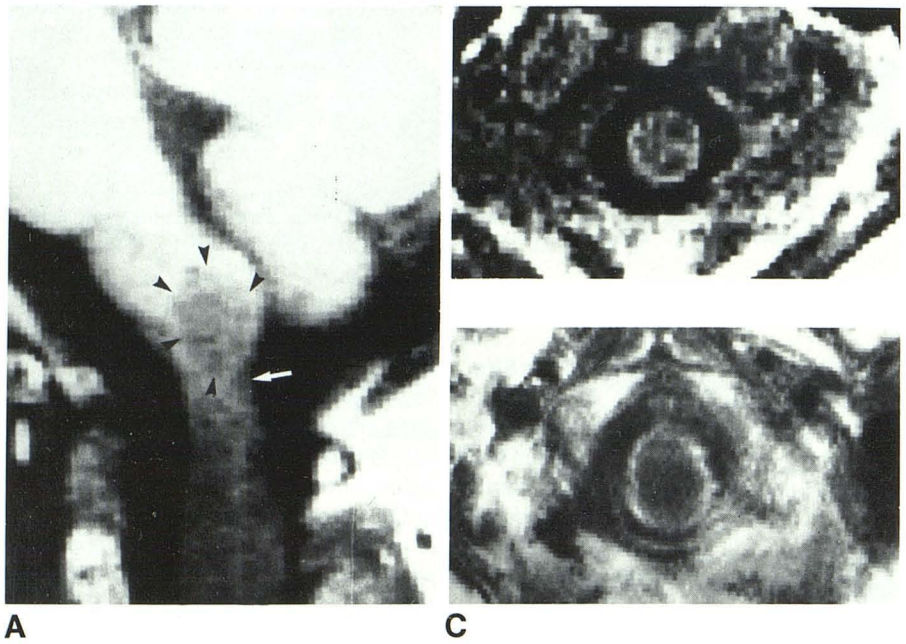

Fig. 12.—Glioma. **A**, Sagittal SE 500/30 image. Expansion of medulla due to localized cyst (*arrowheads*). Normal size of medullary cervical junction (*arrow*). Signal of cervical cord cyst is not as low as in uncomplicated cyst. **B**, Axial SE 500/30 image. Inhomogeneous signal within cord cavity compatible with mixed solid/cystic components. **C**, Axial SE 500/30 image of uncomplicated cavity. Homogeneous low signal for comparison.

on the posture of the patient, namely that it collapses in the upright position [2, 15]. This undoubtedly occurs during air myelography, where there is a difference in hydrostatic pressure of fluid inside an intramedullary cavity and the subarachnoid air [1, 2, 21]. This mechanism cannot be used to explain a small cord size, either on metrizamide studies, plain CT scans, or MR images, where the pressures in these spaces are equal. A more plausible explanation would be that the cavity varies in size in different parts of the spinal cord, and atrophy is present in unpredictable regions. Generalized cord atrophy has been a concomitant finding in some cases studied.

Intramedullary Cavities

Intramedullary cavities have been divided into hydromyelia, which is a dilatation of the central canal, often communicating

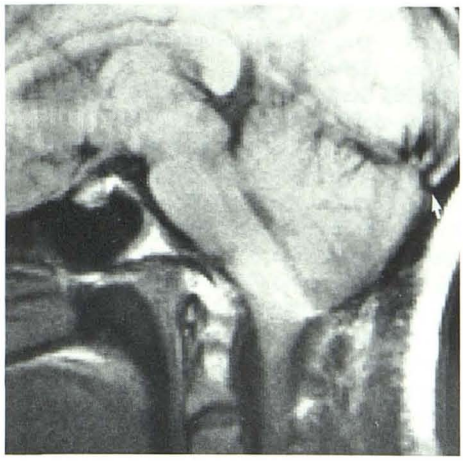

Fig. 13.—Sagittal SE 500/30 image. Caudal extension of cerebellar tonsils and hemispheres through occipital craniectomy (*arrow*). Compression of fourth ventricle.

with the ventricular system, and syrinx, arising primarily outside the central canal [1, 2, 14]. The latter occurs secondary to intramedullary tumors, trauma, and bleeding into the spinal cord [1, 3, 25, 26]. Hydromyelia has been thought variously to arise from interference with the ventricular or subarachnoid pressure and pulsation, in the presence of a Chiari I malformation [1–3, 22–24]. From a therapeutic standpoint, the important factor is to determine whether the cavity communicates with the fourth ventricle and if cerebellar tonsillar ectopia is present.

CT resolution is better in the cervical than thoracic regions: Large cervical spinal cord cavities are occasionally visible on plain axial CT scans, especially when high-resolution scanners are used [7]. Smaller cavities are demonstrated only when they fill with metrizamide. It is unknown what proportion of cavities are thus filled, even with delayed repeat CT examinations. In our series cavities were seen on MR in all cases where the spinal cords were enlarged but only in a fraction of small cords. The reason MR failed to reveal cavities within small spinal cords may well be the small size of the cavities, which are invisible because of partial-volume effect on the 10–15-mm-thick MR sections. Preliminary published data using surface coils and stronger magnets indicate substantial improvement in spatial resolution in examinations of anatomic structures close to the surface, such as the orbit and the temporal bones [27, 28]. SE 500/30 imaging seems to be the optimal technique for demonstrating cavities. It is important to image cord cavities on both sagittal and coronal views. The axial section is sometimes useful in viewing the cavities, especially in the thoracic region, where CT scans are considerably degraded by artifacts. However, because of the limited anatomic field covered by multiple-plane axial sections, it is not possible to view the entire spinal cord using a single set of scans; this method should be reserved for diagnosing cavities that are shown inadequately in the other planes.

Filling of an intramedullary cavity on metrizamide CT does not mean that there is communication with the ventricular system. It has been variously suggested that filling occurs by transependymal/cord passage of contrast material, filling via an open communication with the subarachnoid space at the conus medullaris, or via the fourth ventricle at the obex [15, 26, 29]. The cord cavities may extend into the medulla; some have rounded configurations and appear to enlarge the medulla and distort the fourth ventricle, with which it does not seem to communicate. In other cases the upper margins are tapered, suggesting a small communication with the ventricular system, even though a passage is not seen due to the limited spatial resolution. In other cases the cavities are situated entirely within the cervical and thoracic cord, quite distal to the ventricular opening. The caudal limit of cavities that end in the cervical region are usually clearly demarcated; those that terminate in the thoracic cord are seldom defined due to the poor resolution of our current MR imaging in this location.

As clear communication between intramedullary cavities and the ventricular system is almost never demonstrated, it is not usually possible to differentiate syringomyelia from hydromyelia. Truly eccentric location within the spinal cord may be more characteristic of syringomyelia than of hydromyelia. In our studies, unfortunately, the cavities were usually large and occupied most of the spinal cord. Spinal cord tumors may be partly cystic. The cystic and solid parts of tumors are seen to have different signal intensities; the locations and configurations of the cord expansion may also be eccentric and irregular, as shown in one of our cases. In cases of syrinx associated with a cord tumor the cyst had an appearance identical to simple hydromyelia, but the tumor itself often had abnormal signal on SE 2000/120 images. The relation of the cavities to the tumor was less clear-cut in the case that had been treated by surgery and radiotherapy. It is possible that the latter was the sole cause of the syrinx, since meningioma is rarely associated with syringomyelia [25].

Chiari Malformation

The incidence of the Chiari I malformation in our study was similar to that reported in the literature [1–3, 23, 24]. It is noteworthy that this malformation was present only in cases where the intramedullary cavity was below the medullocervical junction and was not seen in the two cases in which the cyst involved the medulla. The significance of this association is unknown. The incidence of asymptomatic hydromyelia in patients investigated for clinical symptoms of the Chiari I malformation is unknown. The use of MR in the investigation of diverse neurologic disease has already detected some asymptomatic Chiari malformations, and undoubtedly incidental hydromyelia will be revealed. Irrespective of the mechanistic relation of the Chiari malformation to production of hydromyelia, it is generally agreed that it should be treated at the same time as the cord cavity is decompressed [2, 4, 5, 8, 9]. Tonsillar ectopia is detected on sagittal views: the tonsils are sometimes contiguous and inseparable from the posterior margin of the spinal cord, and may be confused with localized tumor expansion of the medulla and cervical cord [30].

Postoperative Changes

Successful decompression of hydromyelia may be evaluated by MR imaging, which reveals changes of spinal cord size. The effects of occipital decompression for the Chiari malformation are also important; in one of our cases, the entire cerebellum and tonsils had herniated downward into the cervical region, through the craniectomy, causing compression of the medulla; this may have accounted for the deterioration in the patient's bulbar symptoms. Normal cord size and failure to reveal an intramedullary cavity, on the other hand, indicate successful decompression.

REFERENCES

1. Barnett HJM, Foster JB, Hudgson P. *Syringomyelia.* London: Saunders, **1973**
2. Logue V. Syringomyelia: a radiodiagnostic and radiotherapeutic saga. *Clin Radiol* **1972**;22:2–16
3. Williams B. On the pathogenesis of syringomyelia: a review. *J R Soc Med* **1980**;73:798–806
4. Schlesinger EB, Autunes JL, Michelson WJ, Louis KM. Hydromyelia: clinical presentation and comparison of modalities of treatment. *Neurosurgery* **1981**;9:356–364
5. Cahan LD, Bentson JR. Considerations in the diagnosis and treatment of syringomyelia and the Chiari malformation. *J Neurosurg* **1982**;57:24–31
6. Taylor CH, Meguro K, Rowed DW. Favorable results with syringosubarachnoid shunts for treatment of syringomyelia. *J Neurosurg* **1982**;56:517–523
7. Gardner WJ, Bell HS, Poolos PN, Dohn DF, Steinberg M. Terminal ventriculostomy for syringomyelia. *J Neurosurg* **1977**; 44:609–617
8. Garcia-Uria J, Leunda G, Carrillo R, Bravo G. Syringomyelia: long-term results after posterior fossa decompression. *J Neurosurg* **1981**;54:380–383
9. Williams B. A critical appraisal of posterior fossa surgery for communicating syringomyelia. *Brain* **1978**;101:223–250
10. Di Chiro G, Axelbaum SP, Schellinger D, et al. Computed axial tomography in syringomyelia. *N Engl J Med* **1975**;292:13–16
11. Forbes W St C, Isherwood I. Computed tomography in syringomyelia and the associated Arnold-Chiari type I malformation. *Neuroradiology* **1978**;15:73–78
12. Rinaldi I, Kopp JE, Harris WO, et al. Computer assisted tomography in syringomyelia. *J Comput Assist Tomogr* **1978**;2:633–635
13. Bonafe A, Ethier R, Melancon D, Belanger G, Peters T. High resolution computed tomography in cervical syringomyelia. *J Comput Assist Tomogr* **1978**;2:42–47
14. Pullucino P, Kendall BE. Computed tomography of 'cystic' intramedullary lesions. *Neuroradiology* **1982**;23:117–121
15. Aubin ML, Vignaud J, Jardin C, Bar D. Computed tomography in 75 clinical cases of syringomyelia. *AJNR* **1983**;2:199–204
16. Bonafe A, Manelfe C, Espagno J, Guiraud B, Rascol A. Evaluation of syringomyelia with metrizamide computed tomographic myelography. *J Comput Assist Tomogr* **1980**;4:797–802
17. DeLaPaz RL, Brady TJ, Buonanno FS, et al. Nuclear magnetic resonance (NMR) imaging of Arnold-Chiari type I malformation with hydromyelia. *J Comput Assist Tomogr* **1983**;7:126–129
18. Norman D, Mills CM, Brant-Zawadzki M, Yeates A, Crooks LE, Kaufman L. Magnetic resonance imaging of the spinal cord and canal: potentials and limitations. *AJNR* **1984**;5:9–14, *AJR* **1983**;141:1147–1152
19. Han JS, Kaufman B, EL Yousef SJ, et al. NMR imaging of the spine. *AJNR* **1983**;4:1151–1159, *AJR* **1983**;141:1137–1145
20. Modic MT, Weinstein MA, Pavlicek W, Boumphrey F, Starnes D, Duchesneau PM. Magnetic resonance imaging of the cervical spine: technical and clinical observations. *AJNR* **1984**;5:15–22, *AJR* **1983**;141:1129–1136
21. Westberg G. Gas myelography and percutaneous puncture in the diagnosis of spinal cord cysts. *Acta Radiol [Suppl]* (Stockh) **1966**;252
22. Gardner WJ. The dysraphic states from syringomyelia to anencephaly. Amsterdam: Excerpta Medica, **1973**
23. Du Boulay G, Shah SH, Currie JC, Logue V: The mechanism of hydromyelia in Chiari type I malformations. *Br J Radiol* **1974**;47:579–587
24. Newmaan PK, Terenty TR, Foster JB. Some observations on the pathogenesis of syringomyelia. *J Neurol Neurosurg Psychiatry* **1981**;44:964–969
25. Blaylock RL. Hydrosyringomyelia of the conus medullaris associated with a thoracic meningioma. *J Neurosurg* **1981**;54:833–835
26. West RJ, Williams B. Radiographic studies of the ventricles in syringomyelia. *Neuroradiology* **1980**;20:5–16
27. Schenck JF. *Magnetic resonance imaging of the orbit.* Milwaukee: General Electric, **1984**
28. Daniels DL, Pech P, Haughton VM. *Magnetic resonance imaging of the temporal bone.* Milwaukee: General Electric, **1984**
29. Winkler SS, Sackett JF. Explanation of metrizamide brain penetration: a review. *J Comput Assist Tomogr* **1980**;4:191–193
30. Wickbom I, Hanafee W. Soft tissue anatomy within the spinal canal as seen on computed tomography. *Radiology* **1980**;134:649–655